NASA Technical Memorandum 107462
AIAA–97–1609

Comparison of Predicted Low Speed Fan Rotor/Stator Interaction Modes to Measured

Daniel L. Sutliff
AYT Corporation
Brook Park, Ohio

James Bridges
Lewis Research Center
Cleveland, Ohio

Edmane Envia
NYMA, Inc.
Brook Park, Ohio

Prepared for the
3rd Aeroacoustic Conference
cosponsored by the American Institute of Aeronautics and Astronautics
and the Confederation of European Aerospace Societies
Atlanta, Georgia, May 12–14, 1997

National Aeronautics and
Space Administration

COMPARISON OF PREDICTED LOW SPEED FAN ROTOR/STATOR INTERACTION MODES TO MEASURED

Daniel Sutliff*
AYT Corporation
Brook Park, Ohio 44142

James Bridges*
National Aeronautics and Space Administration
Lewis Research Center
Cleveland, Ohio 44135

Edmane Envia*
NYMA, Inc.
Brook Park, Ohio 44142

Abstract

The *V072 Rotor Wake/Stator Interaction Code* is widely used as a state-of-the-art prediction code. This paper validates the code by comparing experimentally measured mode levels to those predicted by V072. The experimental mode levels were measured by the Rotating Rake system installed on the 48 inch Active Noise Control Fan at NASA Lewis Research Center. V072 predicted mode levels by inputting the actual wake profiles of the ANCF rotor measured by a 2-component hotwire. The mode levels were also predicted from the V072 wake models. V072 reasonably predicts the mode levels within the design limits of the code.

Introduction

The periodic interaction of fan viscous wakes with stator vanes is a principal source of tone noise in modern turbofans. This source, referred to as rotor-stator interaction noise, occurs at discrete tones at the harmonics of the blade passing frequency (BPF) and its harmonics. Rotor-stator interaction noise can have a significant impact on the noise exposure problem during takeoff and landing. In view of stringent community noise regulations and NASA's Advanced Subsonic Technology Noise Reduction Program it is highly desirable to have a method to accurately predict the rotor-stator interaction noise.

The *V072 Rotor Wake/Stator Interaction Code* has been used in a number of cases as a preliminary design tool.[1] Currently, the prediction of the in-duct mode levels has not been verified. This paper addresses the question of whether V072 accurately predicts the mode levels within the design limits of the code for a low speed fan.

For this paper, the ANCF rotor wake profiles were obtained using a 2-component hotwire probe. The upwash was computed from the velocity and angle hotwire data. This information was input into V072 which computed the mode power levels (PWLs). These predicted mode PWLs were compared to data obtained experimentally from the rotating rake.

ANCF Test Bed

The Active Noise Control Fan[2,3] (ANCF) uses a 16-bladed variable-pitch rotor and can be configured with stator vanes to provide specific mode generation and propagation for aeroacoustic research. A unique feature on the ANCF is the direct attachment of the rotor centerbody to the rig support column, eliminating the need for struts, which could contaminate acoustic measurements. Additionally, an Inflow Control Device (ICD) allows for static testing. The combination of low tip speed (~400 ft/sec) and the 48 in. diameter produces fan tones of the same frequencies produced by full-size advanced engines. A schematic of the ANCF is shown in Fig. 1.

The primary measurement device on the ANCF is the Rotating Rake.[5] The Rotating Rake is an implementation of a technique originally conceived by T.G. Sofrin whereby a rake containing radially distributed pressure transducers rotates in the circumferential direction at a

*Senior Member, AIAA.

precise fraction of the fan rotational speed. Since each circumferential acoustic mode is known to rotate at a unique speed[4] in the rotor reference frame, a Doppler shift is induced in the rake reference frame. Further reduction of the data into radial modes is accomplished through a least squares curve fit to Bessel basis functions.

The ANCF is located in the NASA LeRC's Aeroacoustic Propulsion Laboratory (APL), a hemispherical anechoic (to 125 Hz) test facility. Farfield measurements are taken from 28 microphones at 50 ft in the ANCF horizontal plane. The SPL data from these microphones are corrected to 40 ft, standard day conditions.

Fan/Duct Modes

The classic paper by Tyler and Sofrin[5] presents the theory of fan-duct mode generation and propagation. The generation of circumferential spinning modes is governed by the following equation:

$$m = sB \pm kV \tag{1}$$

where

m = circumferential mode number,
s = harmonic index,
B = number of rotor blades,
k = an integer (0,1,2,...),
V = number of stator vanes.

The rotor locked mode (k = 0, m = sB) spins at the shaft rotation speed. This mode, and higher order modes, can only propagate in a narrow annular duct if the blade tip speed corresponding to its spin rate is above Mach = 1.0. Lower order modes, which spin faster, may propagate if their spin rate is supersonic. The critical tip Mach number is greater than 1.0 for non-narrow annular ducts. The spin rate of a circumferential mode is determined by the following equation:

$$\Omega_m = \frac{sB\Omega}{m} \tag{2}$$

where

Ω_m = mode rotation speed,
Ω = shaft rotation speed.

Each circumferential mode, m, can have one or more radial modes, n. Mode propagation is dependent on the cut-off frequency, which is unique to each (m,n) combination. This frequency is dependent on geometric parameters and the eigenvalue of the solution to the wave equation in cylindrical coordinates. Below the cut-off frequency the mode will decay exponentially. Above cut-off propagation occurs and acoustic power is transmitted down the duct and into the farfield. The cut-off frequency for zero duct Mach number is given by:

$$f_{co} = \frac{\hat{e}c_o}{\pi D} \tag{3}$$

where

f_{co} = cut-off frequency,
$\hat{e}$ = duct eigenvalue,
c_o = speed of sound,
D = duct diameter.

The bessel function eigenvalue incorporates the duct geometry effects. The cut-off ratio gives the ratio of the mode frequency to its cut-off frequency.

$$\zeta = \frac{f}{f_{co}} = \frac{\pi sB\Omega_m D}{60\hat{e}c_o} \tag{4}$$

One method of generation of these spinning modes is the periodic interaction of the rotor wake impinging on the stator vanes. These are the primary modes of interest in this study.

V072 Rotor Wake/Stator Interaction Code

V072[6] is a package of FORTRAN computer programs which calculates the in-duct acoustic modes excited by a fan/stator stage operating in a subsonic mean flow. Sound is generated by the stator vanes interacting with the wakes of the rotor blades. The code provides outputs of modal pressure and power amplitudes generated by the rotor-wake stator interaction.

The rotor/stator stage is modeled as an ensemble of blades and vanes of zero camber and thickness enclosed within an infinite hard-walled annular duct. The acoustic pressure within the duct is calculated by distributing pressure dipoles on the surface of the stator vanes and calculating the pressure at an arbitrary point within the duct via the normal mode expansion of the Green's function for an annular duct. By this procedure one obtains an infinite series for the sound pressure within the duct. Each term is a normal mode of the duct multiplied by the amplitude of that mode. The amplitude of each propagating mode is computed and summed, with appropriate factors, to obtain the harmonics of sound power within the duct. These calculations are carried through for both upstream and downstream propagating modes.

The wake flow downstream of the rotor is modeled as a small amplitude disturbance flow, superimposed upon a steady mean flow. The mean part of the flow is assumed

to have no radial component, so that the mean flow stream surfaces are cylindrical. It is further assumed that if one of these cylinders is unwrapped to form a plane, the mean flow will be parallel. This is a justifiable approximation as regards the calculation of the forces on the stator vanes provided that the wake parameters chosen are those obtained at the axial station of the stator vanes themselves. The magnitude of the wake flow velocity is constant on lines parallel to the mean flow streamlines, but varies periodically in the direction normal to the mean flow streamlines.

Experimental Measurements

Hotwire

The hotwire data were acquired traversing a probe into the flow radially for different fan speeds. The probe was a "tangential" x-wire having the "x" lying in a plane perpendicular to the radial direction. The probe signals were analyzed to obtain total velocity and tangential (circumferential) flow angle. The circumferential angle of the probes was offset by 40° to compensate for the fan swirl and to keep flow angle fluctuations from occurring outside the valid range for the probe, roughly ±30°. The probe was a TSI model 1246 cross-stream x-wire probe 'upstream type; e.g. the main stem of the probe is kinked 90° to allow the prongs to be oriented normal to, and upstream of, the main stem. The prongs were spaced 60 mils apart and the wire was 0.15 mil diameter platinum coated tungsten. The prongs were reinforced to within 1/4 in. of the wires by epoxy to avoid spurious signal oscillation and sensor breakage by prong vibration. Also, the probe support was reinforced by sliding the 3/16 in. probe support inside of thick-walled 3/8 in. tubing to prevent aeroelastic oscillation of the cantilevered cross-stream support when the probe was inserted the full 16 in. depth.

The hotwire sensors were run with a TSI IFA100 anemometer and the signals were conditioned using the on-board signal conditioners with offset and gain to maximize the dynamic range of the digitizing equipment. Data from the two sensors of the probe were sampled synchronously with the fan by employing a phase-locked angle clock encoder. The encoder was fed a once-per-revolution signal from the fan and output pulses at 1024 samples/rev. The encoder output externally triggered the data acquisition at that rate. The 1/rev signal from the fan was also sampled to assure that data was sampled correctly. The hotwire signals were sampled using the NASA Lewis Digital Acoustic Data System normally used for acquiring acoustic data. This system consists of a CAMAC-based filter/amplifier/digitizer subsystem driven by a Concurrent 9200 workstation which controls the sampling of the data.

The voltages recorded on the workstation were converted to velocities using a polynomial function obtained through in-house calibration procedure. The calibration procedure involves sampling the hotwire signal over a matrix of velocities and angles. Typically 15 velocities (25 to 400 ft/sec) and 13 angles (–30° to 30°) were acquired. A 4th order polynomial was used to fit velocity and flow angle to the sum and difference of the calibration voltages, respectively. This yields a single-valued, smooth function with good sensitivity. Typical errors in the fit were approximately a 0.2° and 2 ft/sec. Both thermal and density compensation were applied using standard corrections.

Data was recorded at each radial location for 100 contiguous revolutions at 1024 points/revolution and converted to instantaneous velocity and angle time records via the polynomial calibration. Velocities and angles were then phase-averaged, first using one fan revolution as an ensemble size, then one blade passage, and finally over all time. The 1/rev signal sampled with the data assured that phase averages were not corrupted by encoder errors in trigger signal generation. Both mean and deviation in each ensemble was produced although only the average blade passage data were used in the V072 prediction procedure.

The data were taken with the hot wire probe located 2.25 in. (1/2 chord) downstream of the rotor trailing edge referenced at the hub. This corresponds to the location of the leading edge of the stator, which was not installed for the hotwire acquisition runs. The radial stations were taken at approximately 3/4 in. increments, except at the tip where more detailed information of the flow was desired. Profiles were taken at 1700, 1750, 1800, and 1850 rpm.

Fan Characteristics

The feature of the ANCF that makes it an unique tool for code validation is its flexibility. Choosing the proper vane combination will result in particular mode combinations to study in isolation. For this study 13, 14, 26, and 28 vanes were configured. Thus the effect of generating a single mode, two radials for a single circumferential mode, or two circumferential modes each with a single radial each can be studied independently.

The modes generated by rotor/stator interaction can be predicted using Eqs. (1) to (3) for the vane counts used in this study. The cut-on modes and their cut-off ratios at $\Omega_c = 1886$ (nominal 100 percent fan speed) are presented in Table I.

Table I: Cut-on Modes at Ω_c =1 886

HARMONIC: VANE COUNT	BPF	2BPF
13	(3,0)	(6,0),(–7,0)
14	(2,0)	(4,0),(4,1)
26	---	(6,0)
28	---	(4,0),(4,1)

The fan rotor has an average chord length of 4.5 in.; 5.31 in. at the hub and 3.68 in. at the tip. The stator vane chord is 4.5 in. Nominal spacing is measured at the hub from the fan blade trailing edge to the stator blade leading edge and was 1/2 chord for this experiment.

Preparation of Hotwire Data for V072 Input

V072 calculates the amplitudes of the duct modes via the Green's function integrals of fluctuating surface pressure distribution on stator vanes. The pressure distribution in turn is related to the upwash on the vanes. The upwash is determined from a description of rotor wake velocity profiles. In the V072 code, these profiles are developed from a set of wake correlations (i.e., wake models), but they can also be specified from velocity measurements acquired downstream of the fan.

When using experimental wake data, however, it is important to specify the upwash information in a manner that is consistent with the assumptions used in the code to construct the wake models. The result of these assumptions (see Refs. 6 and 7 for details) is that any radial flow that might occur downstream of the fan is effectively neglected. Hence, the flow in the rotating frame is envisaged as a tangential wake profile superimposed on a uniform and *parallel* mean flow at each radius. Within the framework of this description, the tangential position of the wake centerline at each radius accounts for any (and all) rotor wake sheet spanwise tilting that might occur due to blade loading and swirl effects. In V072, the tangential position of the wake centerline (at each radius) is determined by the relative flow angle, which is specified as input to the code. This description of the flow is then transformed into a stationary reference frame through the addition of the local wheel speed. From the resulting flow (which remains parallel) vane upwash is computed and used in the subsequent acoustics calculations.

In view of these requirements, measured wake data, which include *non-parallel* flow effects, must be cast in a form consistent with the above parallel flow model. The most physically sensible way to "parallelize" the flow is to mass average the flow angles in both the rotating and stationary frames at each radial measurement station. The resulting mass-averaged flow angle in the rotating frame is then used as the relative flow angle at that radius. Similarly, in the stationary frame, the mass averaged flow angle is used to define the upwash.

Results

Mean Radial Profiles

Complete circumferential averages were calculated on the data at each radial location to obtain the mean velocity or flow angle. These data are shown in Fig. 2. The velocity profile is plotted in Fig. 2(a). the profile is approximately parabolic when away from the hub and tip. Hotwire data were not taken at radii less than 10.5 in. However, earlier data were taken with a total pressure probe at the same location further inward, to about 8.5 in. The velocity computed from total pressure probe had the same profile as that obtained from the hotwire, but the magnitude was about 10 percent lower. This pressure transducer was over-sized and measured the total pressure at a fixed angle, the velocity magnitude is not considered as reliable. However, the profile being nearly identical between the two experiments, the pressure probe velocity from 10.5 to 8.5 in. was applied to enable hotwire velocity extrapolation to those radii. The velocity near the hub drops off rapidly to very low flow.

The flow angle at the stator leading edge is shown in Fig. 2(b). In keeping with the V072 conventions the angles on this plot are referenced with to the tangential direction. Also shown on the plot is the angle at the trailing edge of the rotor as predicted by a streamline curvature code. The flow leaves the trailing edge of the rotor deflected toward the pressure side of the blade due to loading, as expected.

The mean swirl angle is shown in Fig. 2(c). This angle was computed from the mass averaged flow angle and is referenced to the duct centerline. The swirl angle is very nearly linear except near the tip. The stator vane stagger angle is also plotted on Fig. 2(b). The stagger angle is defined as an average of the stator leading and trailing edge metal angles, weighted to the leading edge. This comparison indicates that the stator vanes are at a relatively high incidence angle, and may be separated in the fan.

Blade Averaged Circumferential Profiles

The important part of the data is the 16-blade averaged profiles. The wakes from each of the 16 blades are averaged to obtain a single wake profile. This averaged profile is then assumed to generated by each blade because V072 assumes the wake of each blade is uniform. The upwash calculated is shown on Fig. 3(a) for 2 blade passages. This is for a fan speed of 1850 rpm. Little difference is seen at the other speeds and is not presented here. The profiles appear to be nearly Gaussian. The strongest wake deficits are seen near the center of the blade, with the deficit

decreasing as the radius increases. Very near the hub, (within 2 in.) the deficit is wider and shallower.

The upwash is normalized and "parallelized," as described in the previous section, in Fig. 3(b). This shows the influence of the rotor speed. Figure 4 shows the same data in a shaded contour plot. The wake deficit and swirl angle are qualitatively seen in this format.

Comparison of Experimental to Predicted Mode Levels

Absolute levels. The mode power levels (PWLs) as predicted by V072 using the hotwire wake data were compared to the PWL measured by the rotating rake. V072 was also run using the wake correlation model subroutines to predict the mode levels. The wake model used was loaded fan wake with a Gaussian profile. In general, using the actual wake data appear to have slight benefit. However, keep in mind that the parameters for wake integration were chosen only after comprehensive analysis of the experimental results.

The simplest case is a single mode at BPF. The only cut-on mode with 13 vanes installed is the (3,0) mode. Figure 5 compares the predicted V072 PWL for mode (3,0) to that measured by the rotating rake. Keep in mind the rotating rake measured the PWL near the inlet entrance plane (s=0.0) or near the exhaust exit plane (s=0.5), while V072 predicts the levels at the stator plane (s = 0.3).

The sum of the forward and aft propagating mode PWLs are presented in Fig. 5(a). The agreement between the V072 prediction and the measured levels is excellent. The difference is 0.3 dB at 1700 rpm and –1.2 dB at 1800 rpm. A positive number indicates that V072 overpredicted the mode PWL.

The individual PWLs for the forward and aft directions are shown in Figs. 5(b) and (c), respectively. The predictions are very good. The trend is noticed that V072 tends to predict a flat response with increasing fan speed, while the actual levels tend to increase slightly. In the exhaust the agreement is best at 1700 rpm where V072 underpredicts the level by only 0.9 dB.

Two circumferential modes with a single radial mode each are generated at 2BPF with the 13 vanes. These are the (6,0) and (–7,0) modes and are shown in Figs. 6 and 7. Figure 6(a) compares the total sum of mode PWL generated at 2BPF. The accuracy of the prediction is less consistent. The agreement is very good at 1700, poor at 1800, and fair at 1850 rpm. Looking at the individual duct directions, but still considering the sum of the (6,0) and (–7,0) modes levels, does not indicate a possible reflection problem as with BPF. Further separating the mode PWLs into individual modes and directions, as in Figs. 7(a) to (d) shows no clear trend with mode, or speed. In general V072 predicts benign trends with speed, i.e. a nearly linear decrease in PWL with increasing RPM. This is not the case with the measured fan levels. Large mode PWL changes with speed are seen in both modes and directions. Since the changes in wake profiles as a function of fan speed as measured by the hotwire were also benign the reason for the disagreement in the predicted levels is likely not a result of the mode generation at the source. It is likely due to other factors discussed in the next section.

Figure 8 presents the (2,0) mode PWL generated at BPF the interaction of 16 blades with 14 vanes. V072 significantly underpredicted the total PWL by about 5 dB as noted in Fig. 8(a). Looking at individual directions, in Figs. 8(b) and (c) it is seen that the major discrepancy is attributed to the difference in the exhaust. V072 under predicts the level in the exhaust by about 7 dB. The difference in the inlet is better, about 2 dB. The trend with speed is good in both directions.

At 2BPF the 14 vane configuration generates a single circumferential mode with two radials; (4,0) & (4,1). The total PWL is accurately predicted as noted on Fig. 9(a). The best agreement is at 1700 rpm: –1.2 dB. The sum of (4,0) & (4,1) PWL mode levels for the separate duct directions shows fair agreement in the inlet (Fig. 9(b)). The difference is about –2.8 dB at 1700 to about –5.4 dB at 1850 rpm. Examining the exhaust PWL shows excellent agreement. The difference is less than 0.5 dB, except where V072 does not predict the PWL drop at 1850 rpm.

The PWL of the individual radials are shown in Figs. 10(a) to (d). This could be considered the most challenging case for a prediction. Indeed it is hard to make a definitive statement. Measured by the rotating rake the (4,0) mode is significantly lower than the (4,1); as much as 10 to 20 dB lower. The much lower (4,0) mode level also has significant variation. Considering the physical fan levels, this variation in the lower level of two modes, is expected. Small fluctuations in the strong (4,1) mode will cause seemingly large variations in the weaker (4,0) mode. V072 does predict the (4,1) to be stronger than the (4,0) but not as great a difference between these radials. Put another way, the dynamic range of the experimental data is greater than that of the code. The prediction is best at 1700 rpm and for the (4,1) in the exhaust.

The 16 blade, 26 vane interaction cuts-off BPF. Only the (6,0) mode propagates at 2BPF. Figure 11 shows the modal levels for this configuration. The major difference arises from disagreement in the inlet levels. The interesting variation seen in Fig. 11(b) of mode level in the inlet as a

function of speed was commented on previously.[3] To date the exact reason for this variation has not been proven. It is likely not a direct source phenomenon since there is very little qualitative difference in the wakes with speed and therefore it is not expected that V072 should predict this trend. The exhaust PWL predictions for the (6,0) mode are very accurate as shown on Fig. 11(c).

BPF was also cut-off for the interaction at with 28 vanes. The modes at 2BPF are (4,0) & (4,1). Figure 12(a) shows that the total PWL produced by the fan is accurately predicted by V072. The inlet levels are over protected by about 1 dB and the exhaust levels are under predicted by 1 to 3 dB (see Figs. 12(b) and (c)). The individual radial mode levels are compared on Fig. 13. The predictions are much better than for 14 vanes. This may be due to the fact that the (4,1) mode, while still greater than (4,0), the difference is not as dramatic. The (4,1) is about 5 dB higher than the (4,1). V072 does a better job of predicting this case. The single exception may be the inlet (4,0) PWL at 100 rpm noted in Fig. 13(a). This drop in the PWL from 1800 to 1700 may be a destructively interfering reflection form the stronger exhaust mode. Unlike the 13 vane case, experimental data to confirm this not were not taken.

The 3BPF results are not significant due to the very low levels produced by the fan.

Relative levels. Another way to determine the validity of the code predictions is to compare trends. A trend analysis that has application to the design process is to compare the change in mode power levels between different vane counts. This trend analysis is done by choosing a vane count as a reference and comparing mode amplitude levels to other vane counts. This is done for the V072 prediction and for the rotating rake data and plotted on a bar graph for two fan speeds. If the height of the two adjacent bars is similar, it means the code prediction of the increment agrees with that obtained experimentally.

Figure 14 compares BPF mode PWLs increments. The amplitude of the (3,0) mode generated by 13 vanes is subtracted from the amplitude of the (2,0) mode generated by 14 vanes.

Figure 14(a) shows the increments for the total PWL generated by the fan. V072 exaggerates the increments at the two speeds shown. This trend is also noted in the inlet and exhaust as seen in Figs. 14(b) and (c).

At 2BPF other trend comparisons can be made. Figure 15 compares increments in the sum of the mode PWLs. Thirteen vanes was arbitrarily chosen as the reference.

The increment in total PWL at 2BPF is shown in Fig. 15(a). The trend with vane count is very good. Figures 15(b) and (c) show the total mode PWL increments for the inlet and the exhaust, respectively. In the inlet V072 predicts the direction of the increment, but exaggerates the level. It is seen that the majority of the 28–13 vane increment is due to the inlet disagreement. The exhaust increments are good, except for 26–13 vanes.

Vane counts of 28 versus 14 vanes, and 26 versus 13 vanes are matching pairs because in each case identical modes at 2BPF are produced. The higher vane counts cut-off BPF.

Figures 16(a) and (b) show the increments in the (6,0) mode when comparing 26 to 13 vanes. These increments are predicted very well. This is surprising when one considers the strange trend with speed noted when looking at the absolute levels of the modes measured by the rotating rake discussed earlier (Fig. 11).

The radial mode trend prediction is shown on Fig. 17. For each radial mode, the mode PWL amplitude from 14 vanes was subtracted from that obtained by with the 28 vane configuration.

Figures 17(a) and (b) show the increments in (4,0) for the inlet and the exhaust. The trend prediction was not very good. The inlet trend is in the wrong direction at 1700 rpm. In the exhaust, the data shows much greater variation than was predicted by V072. Figures 17(c) and (d) show the increments for the (4,1) radial. These trends are accurately predicted by V072.

Discussion

In general the V072 accurately predicted the mode levels. The best results were obtained when considering the overall fan PWL. The individual modes were predicted most accurately in the exhaust.

The more accurate exhaust predictions may be due to the fact that the transition from the hub-to-tip ratio at the rotor-stator plane to the rotating rake measurement plane is less severe in the exhaust than in the inlet. This transition is from s = 0.3 to 0.5 in the exhaust and from s = 0.3 to 0.0 in the inlet. The transition from the annulus to a cylinder may be fundamentally different.

Duct propagation may cause some differences. The Eversman radiation code has been run propagating a few test case modes unit amplitudes. In particular it was noted that at 1700 rpm (= 1.9) the (2,0) mode level increased

2 dB when propagated from the fan face to the exhaust rotating rake measurement location, indicating a reflection or standing wave. No PWL change was noted when the (2,0) was propagated to the inlet measurement location.

Other possible explanations for the inaccurate predictions may be due to a reflection of the exhaust mode as a result of the ramp transition interfering with the inlet. This has been experimentally verified for the 13 vane case in the inlet for BPF.

Also, the flow over the stator blades may be separated. V072 does not model this.

Unfortunately, none of these explanations is likely the dominant reason for the unique and dramatic variation in the (6,0) mode generated by 26 vanes. For example, the Eversman radiation code run with a unit (6,0) mode amplitude showed no variation when propagated to the fore and aft measurement locations. The exhaust PWL is not significantly higher than the inlet so it is not a physical reflection from the exhaust.

A recent phenomenon noted is mode trapping and scattering.[8] This was beyond the scope of this paper, but should be investigated further.

Conclusions

The *V072 Rotor Wake/Stator Interaction Code* predicted the in-duct model levels of the ANCF, a low-speed fan, within the limits of the code. Naturally the effects of propagation and reflection are not accounted for. A variety of mode combinations were predicted fairly well, with one vane configuration being a notable exception.

It is clear from the data that the wake correlation capabilities of V072 are adequate and the primary emphasis should be on mode propagation.

Specific conclusions:

- V072 predicts absolute levels fairly well,
- V072 predicts total PWL better than individual modes,
- V072 predicts generally the direction of vane count trends but exaggerates the increment,
- The V072 wake correlation model provide similar results to those obtained using actual wake data
- Most of the inaccurate predictions are probably due to duct propagation effects

It is recommended that the hotwire and rotating rake data from this experiment be used in a code that would include the effects from coupling, refection, and duct propagation.

References

1. Envia, E, Huff D.L. and Morrison, C.R., "Analytical Assessment of Stator Sweep and Lean in Reducing Rotor-Stator Tone Noise," AIAA-96–1791, May 1996.
2. Heidelberg, L.H., Hall, D.G., Bridges, J.E. and Nallasamy, M., "A Unique Ducted Fan Test Bed for Active Noise Control and Aeroacoustics Research," NASA TM–107213, May 1996, also AIAA-96–1740 May 1996.
3. Sutliff, D.L., Nallasamy, M., Heidelberg, L.J. and Elliott, D.M, "Baseline Acoustic Levels of the NASA Active Noise Control Fan Rig," NASA TM–107214, May 1996, also AIAA-96–1745, May 1996.
4. Hall, D.G., Heidelberg, L. and Konno, K., "Acoustic Mode Measurements in the Inlet of a Model Turbofan using a Continuously Rotating Rake: Data Collection/ Analysis Techniques," NASA TM–105963, Jan. 1993; also AIAA-93-0599, Jan. 1993.
5. Tyler, J.M. and Sofrin, T.G., "Axial Flow Compressor Studies," *SAE Transactions*, Vol. 70, 1962, pp. 309–332.
6. Meyer, H.D. and Envia, E. "Aeroacoustic Analysis of Turbofan Noise Generation," NASA CR–4715, March 1996.
7. Topol, D.A, and Matthews, D.C., "Rotor Wake/Stator Interaction Noise Prediction Code: Technical Documentation and User's Manual," NASA Lewis Research Center, April 1993.
8. Hanson, D.B., "Acoustic Reflection and Transmission of Rotors and Stators Including Mode and Frequency Scattering," AIAA-97–1610, May. 1997.

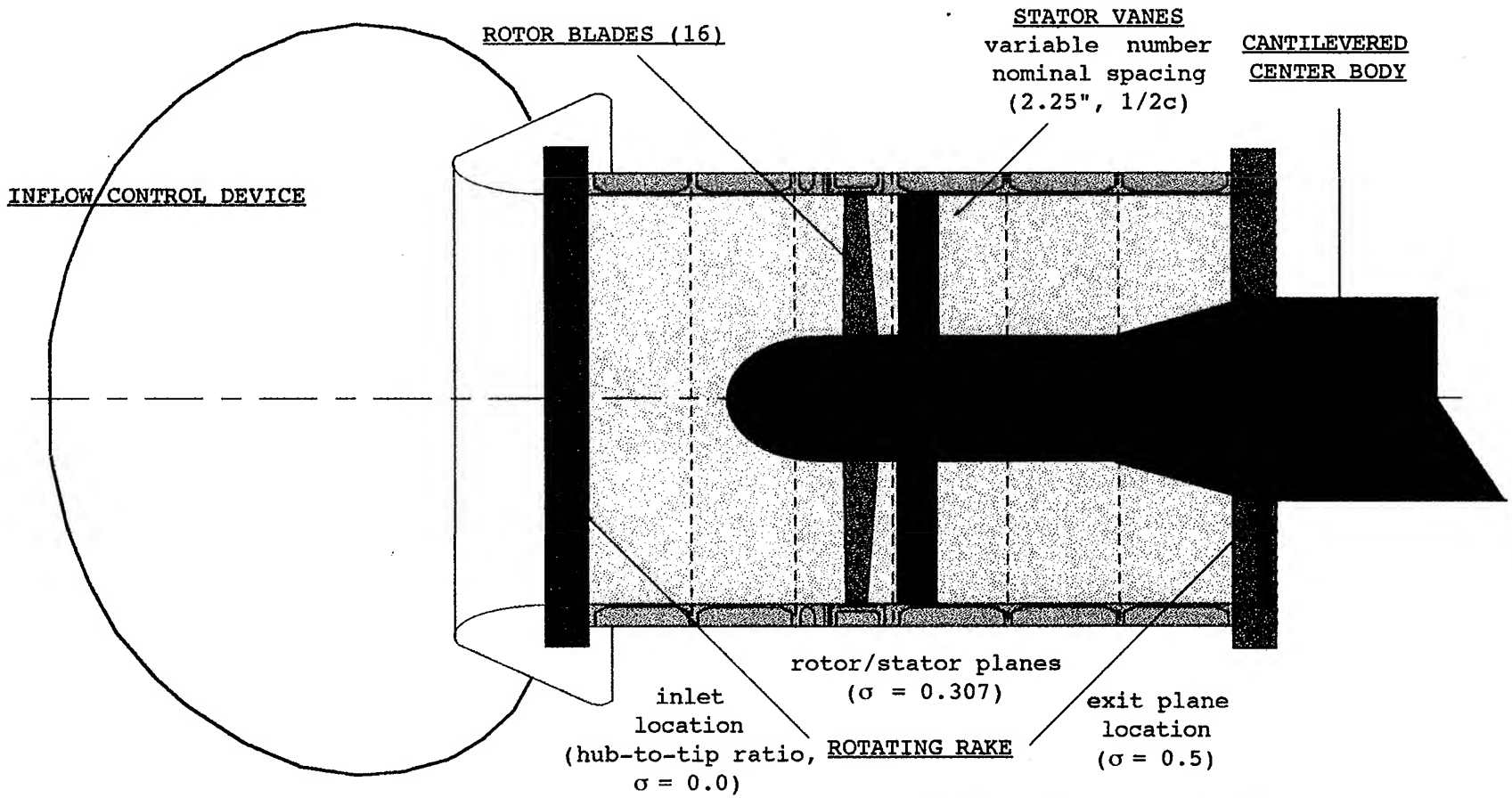

FIGURE 1. Schematic of Active Noise Control Fan showing Measurement Locations

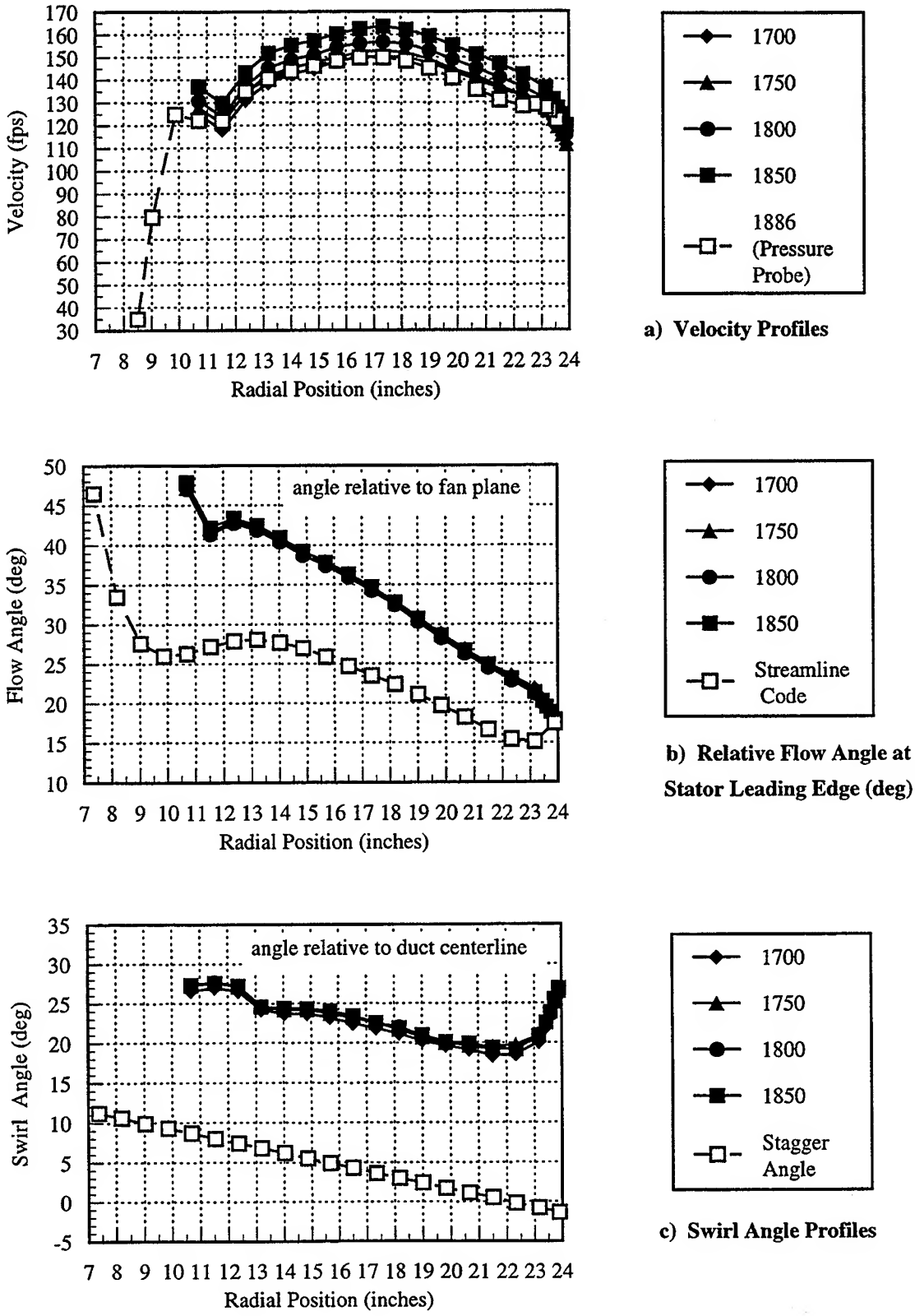

FIGURE 2. ANCF Radial Profiles at 2.25" Downstream from Rotor Plane

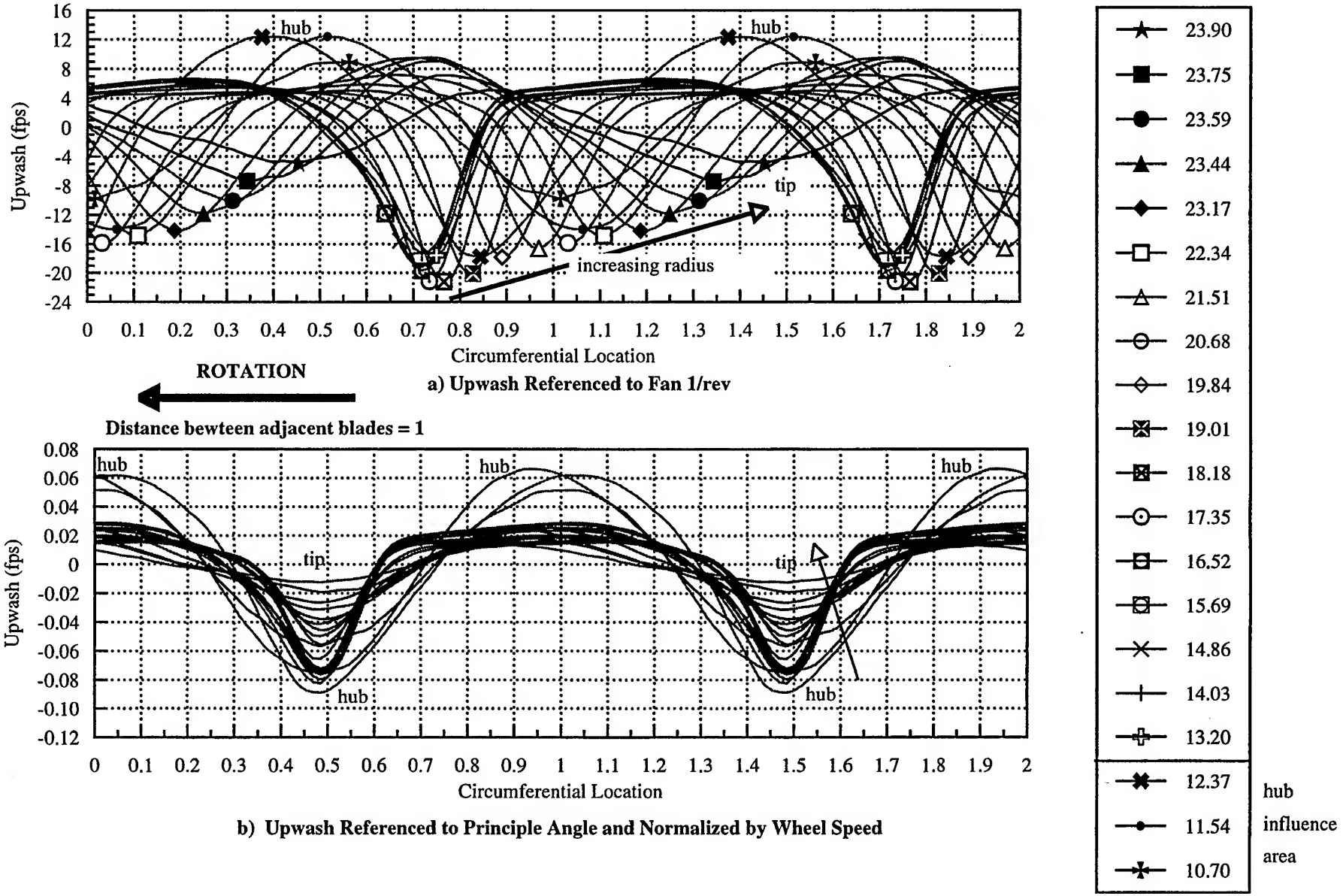

FIGURE 3. Upwash at Stator Vane Leading Edge vs Circumferential Positon

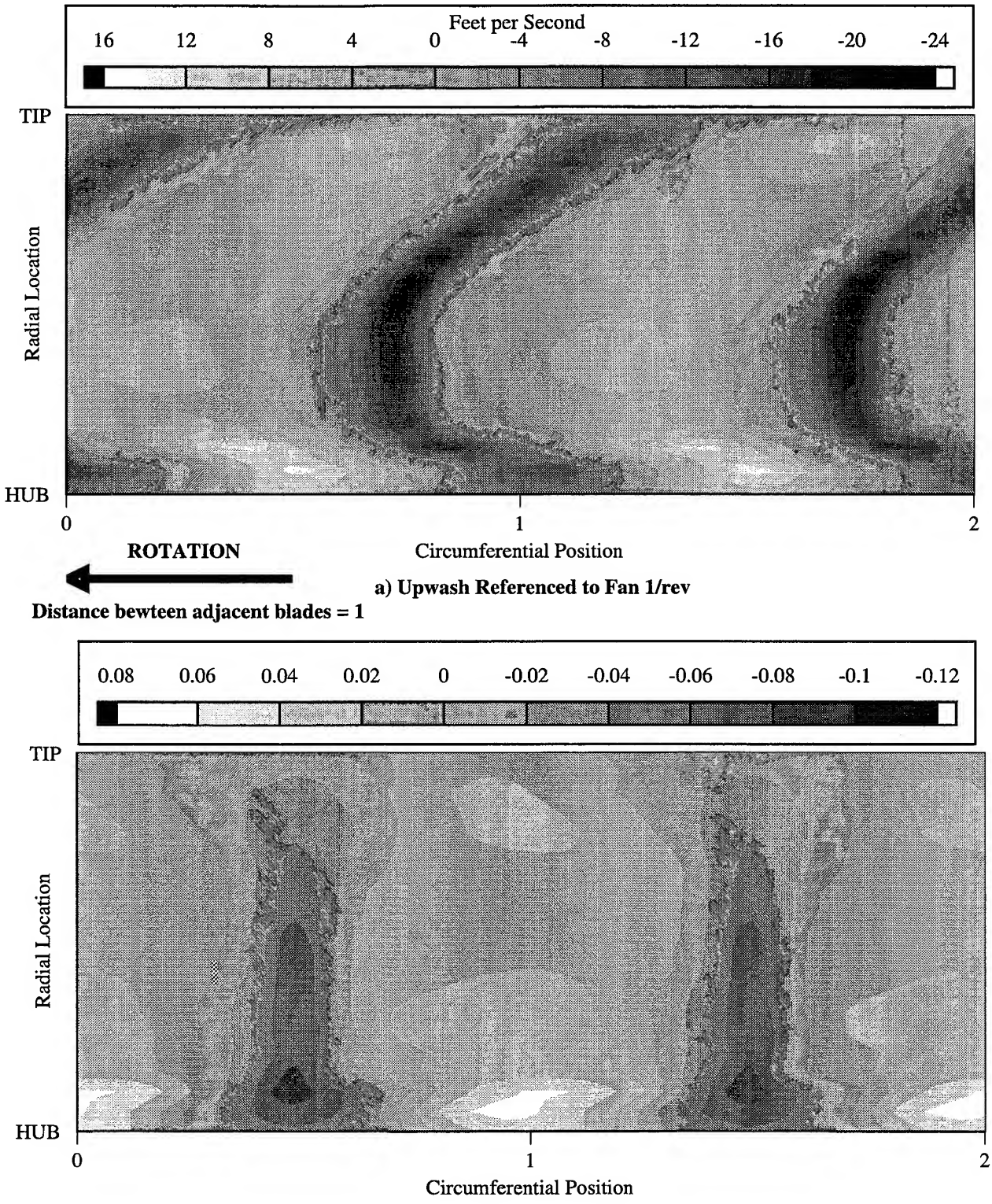

FIGURE 4. Upwash at Stator Vane Leading Edge vs Circumferential Positon

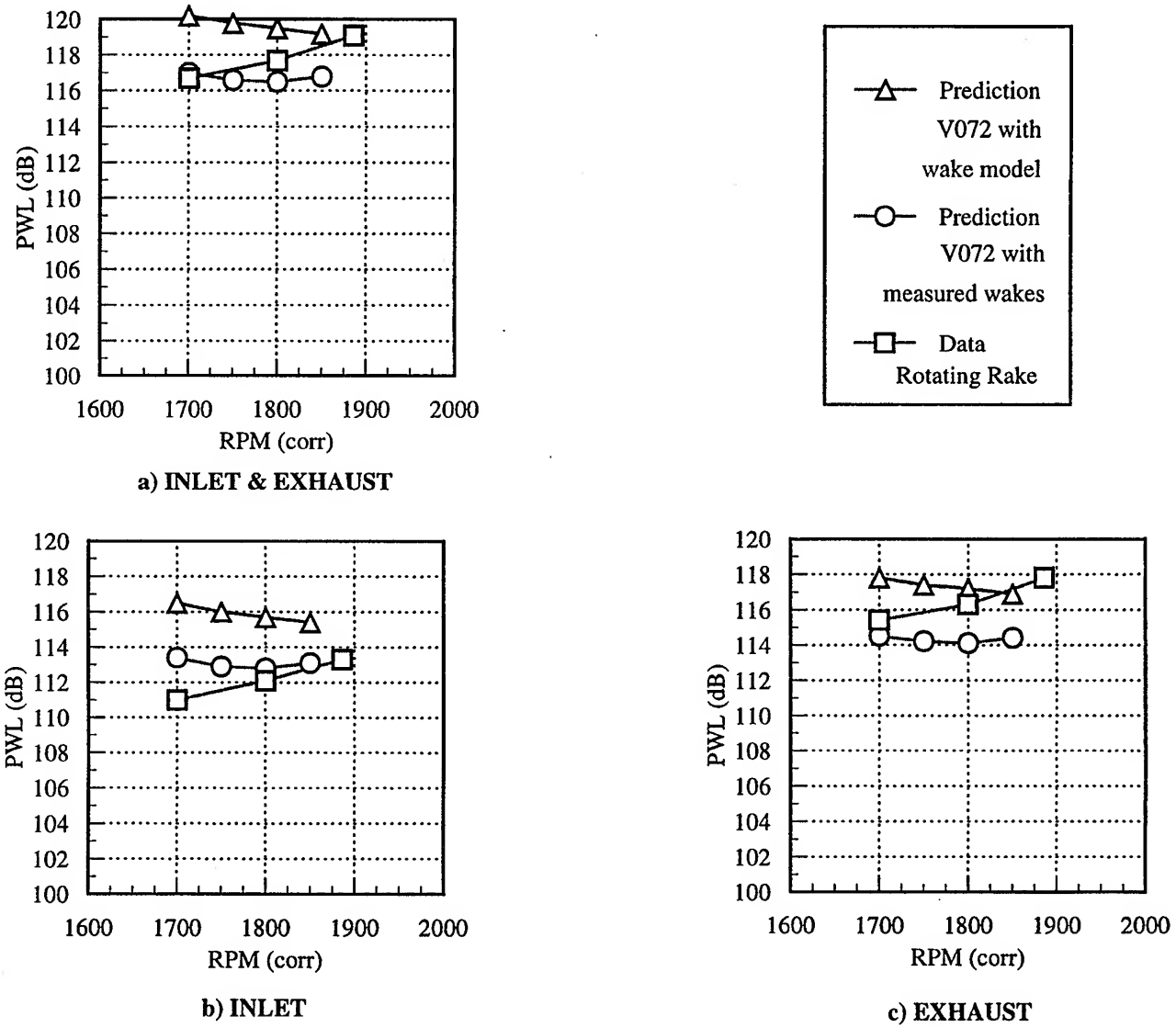

FIGURE 5. Comparisions of Mode Power Levels for 13 Vanes BPF Mode (3,0)

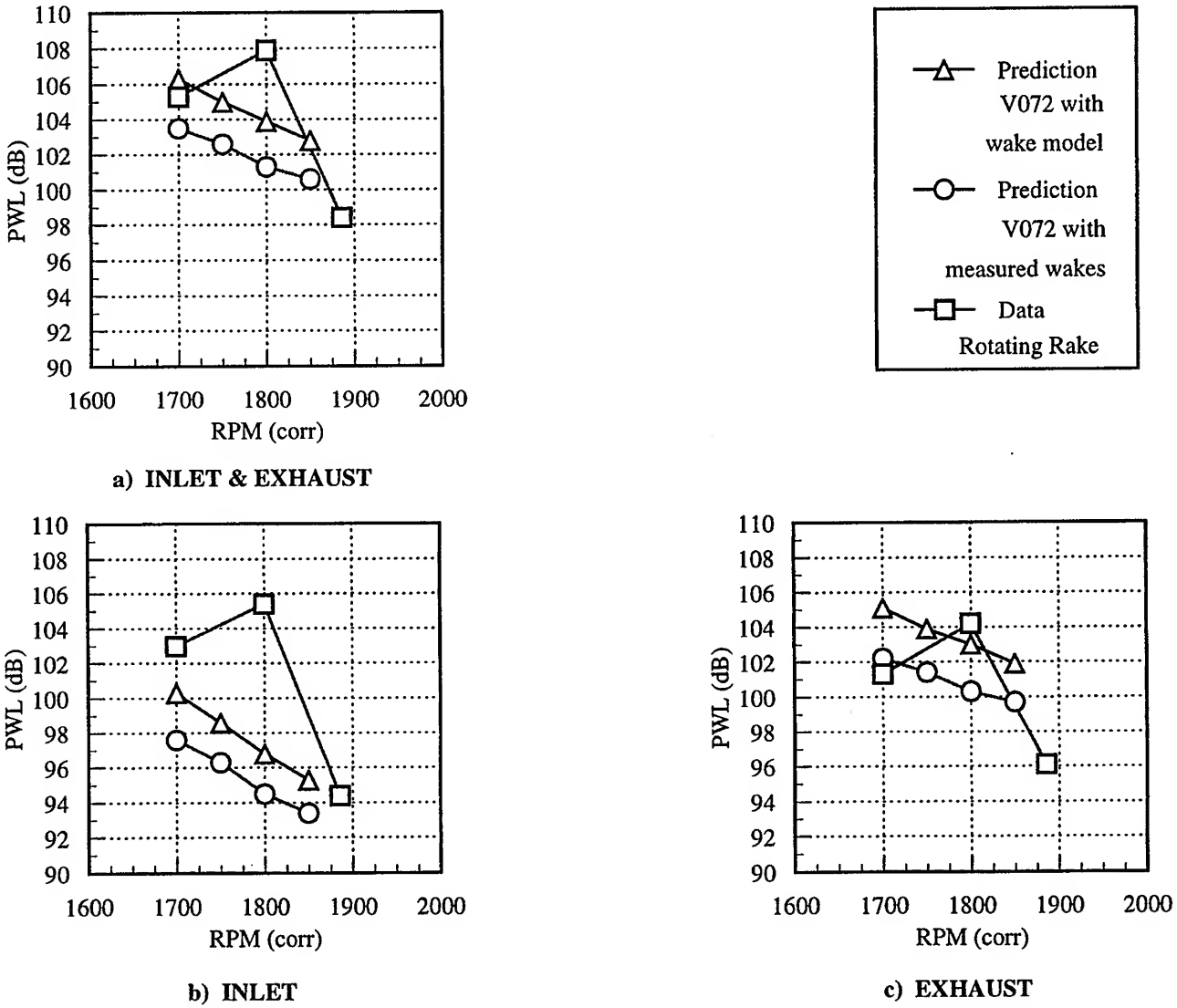

a) INLET & EXHAUST

b) INLET

c) EXHAUST

FIGURE 6. Comparisions of Mode Power Levels for 13 Vanes Sum of 2BPF Modes (6,0) & (-7,0)

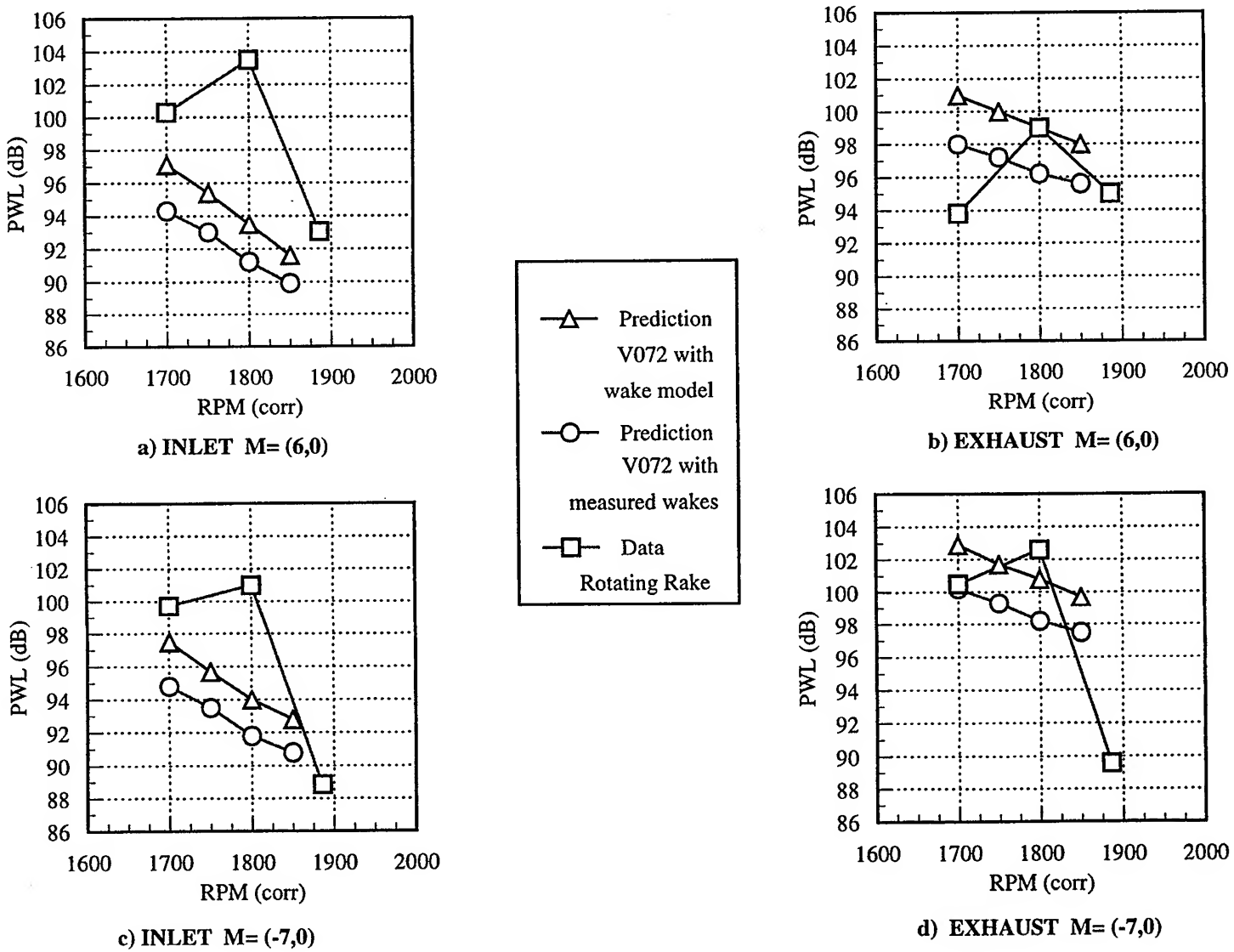

FIGURE 7. Comparisions of Mode Power Levels for 13 Vanes 2BPF Individual Modes (6,0) & (-7,0)

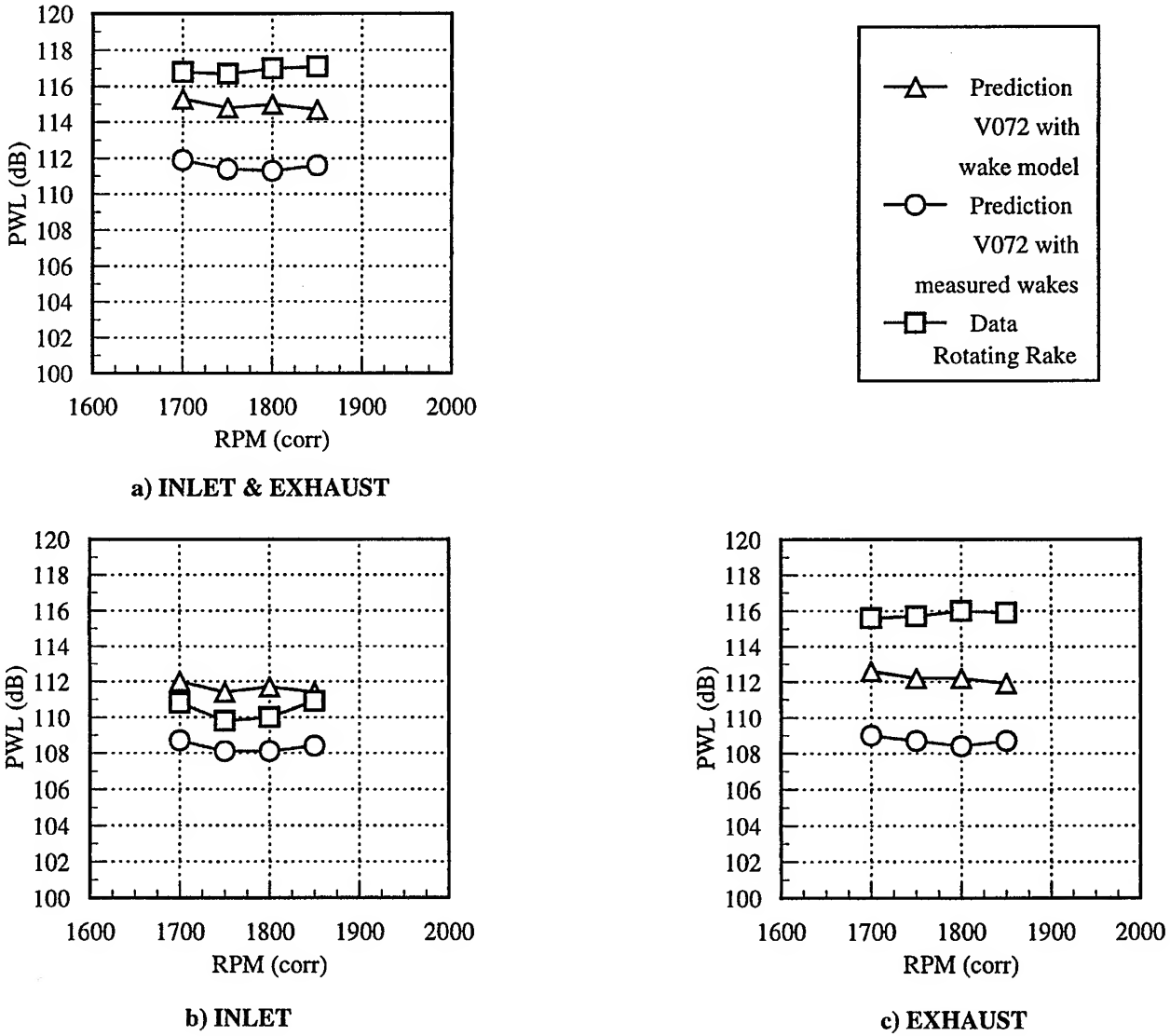

FIGURE 8. Comparisions of Mode Power Levels for 14 Vanes BPF Mode (2,0)

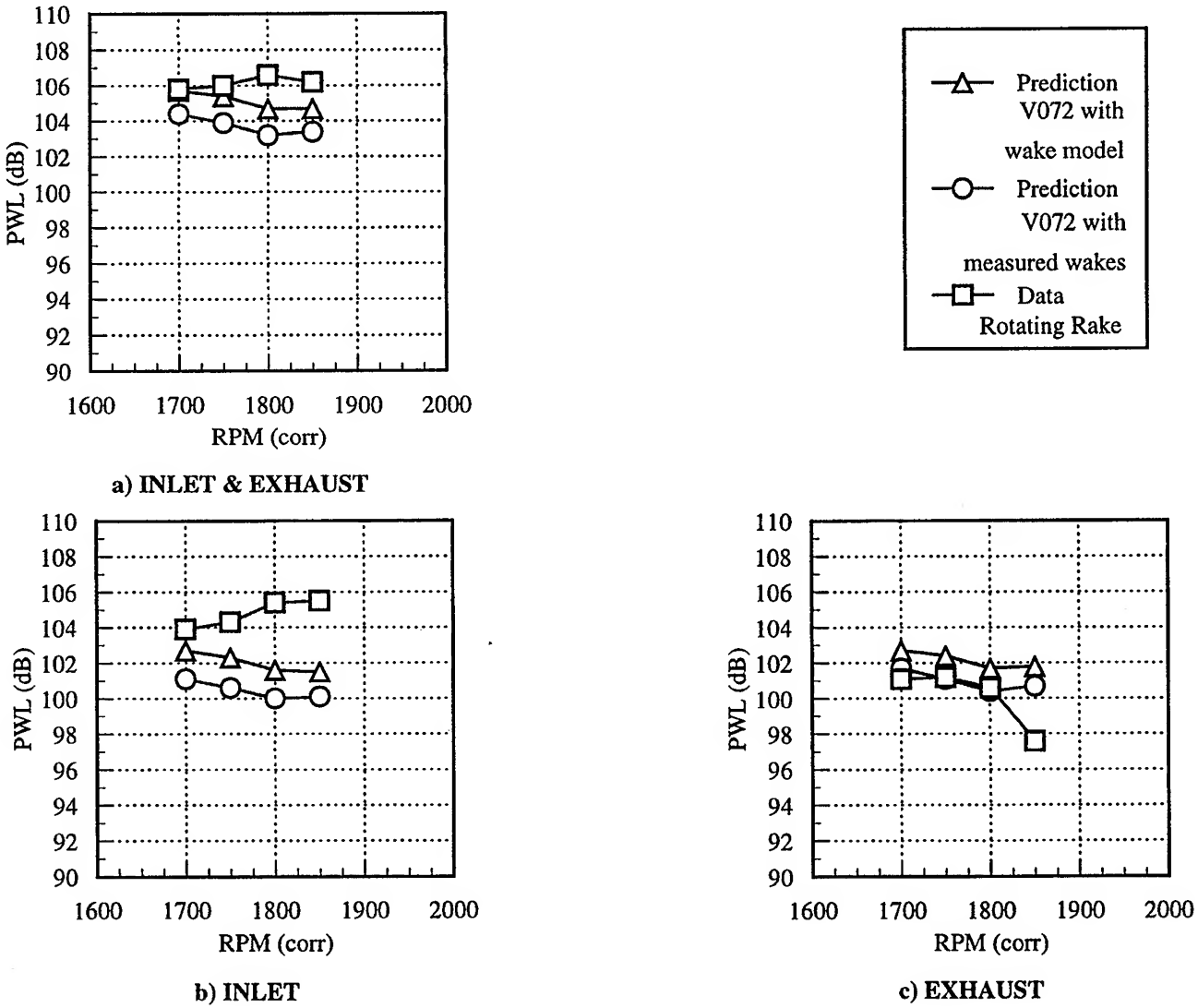

FIGURE 9. Comparisions of Mode Power Levels for 14 Vanes Sum of 2BPF Modes (4,0) & (4,1)

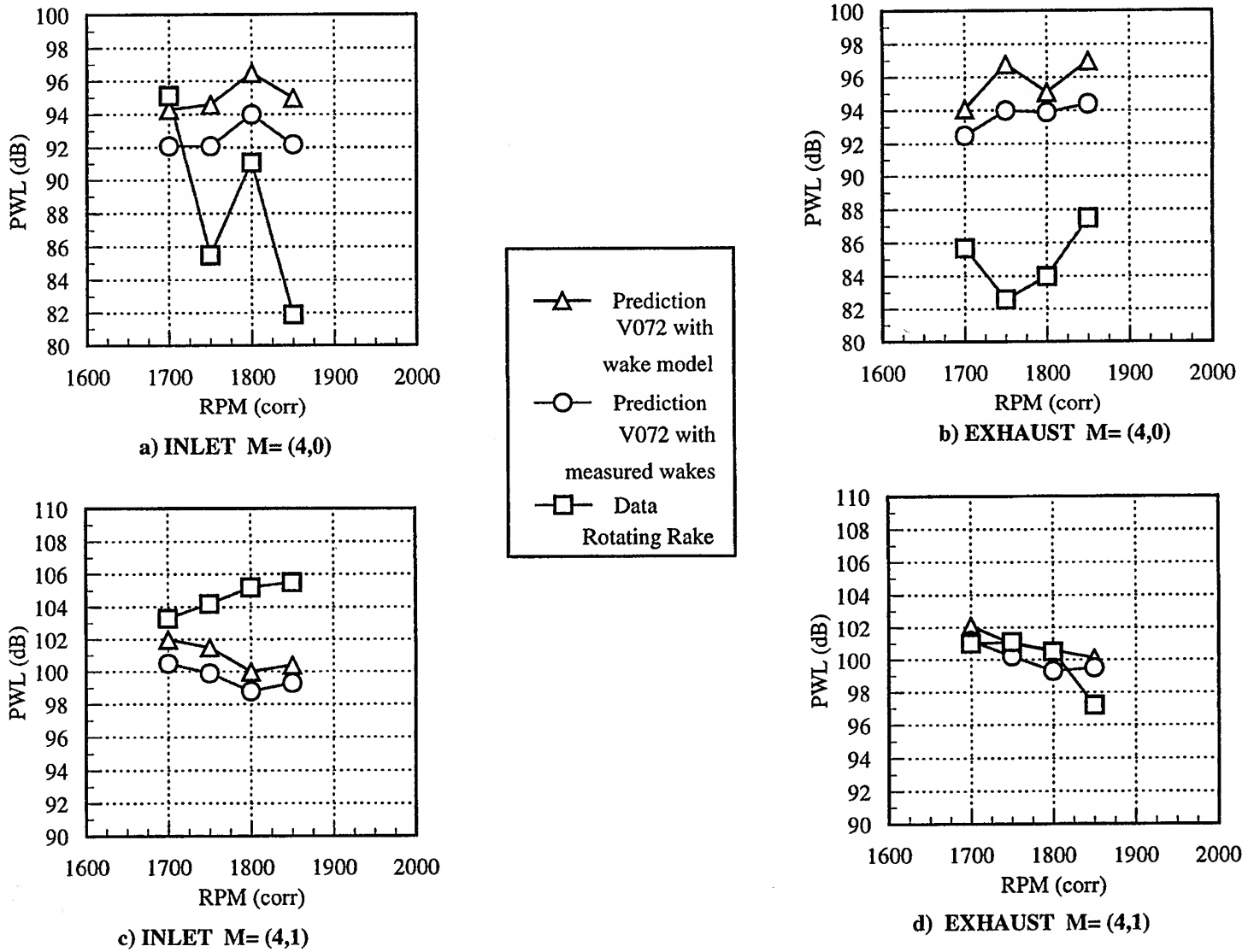

FIGURE 10. Comparisions of Mode Power Levels for 14 Vanes 2BPF Individual Modes (4,0) & (4,1)

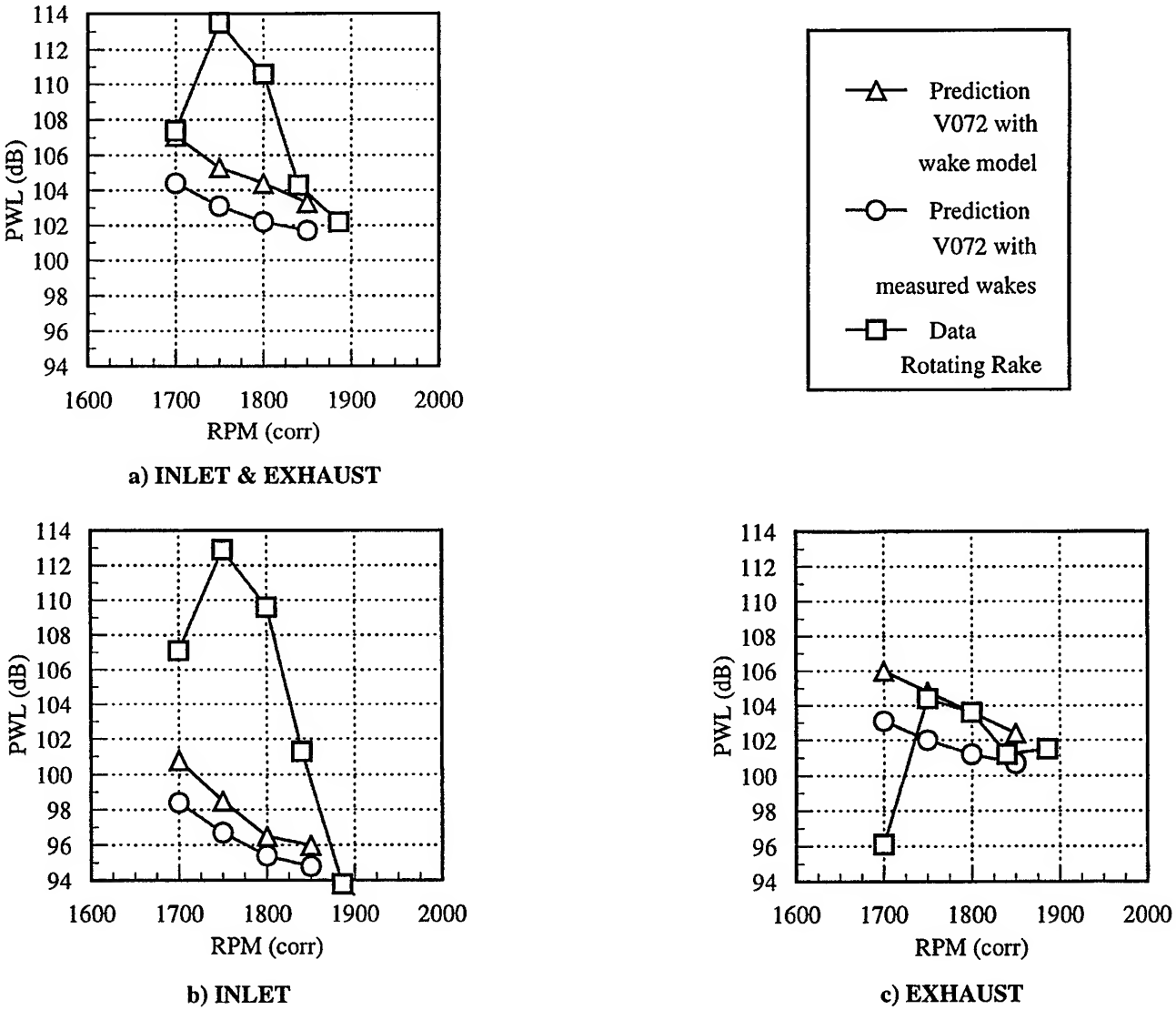

FIGURE 11. Comparisions of Mode Power Levels for 26 Vanes 2BPF Mode (6,0)

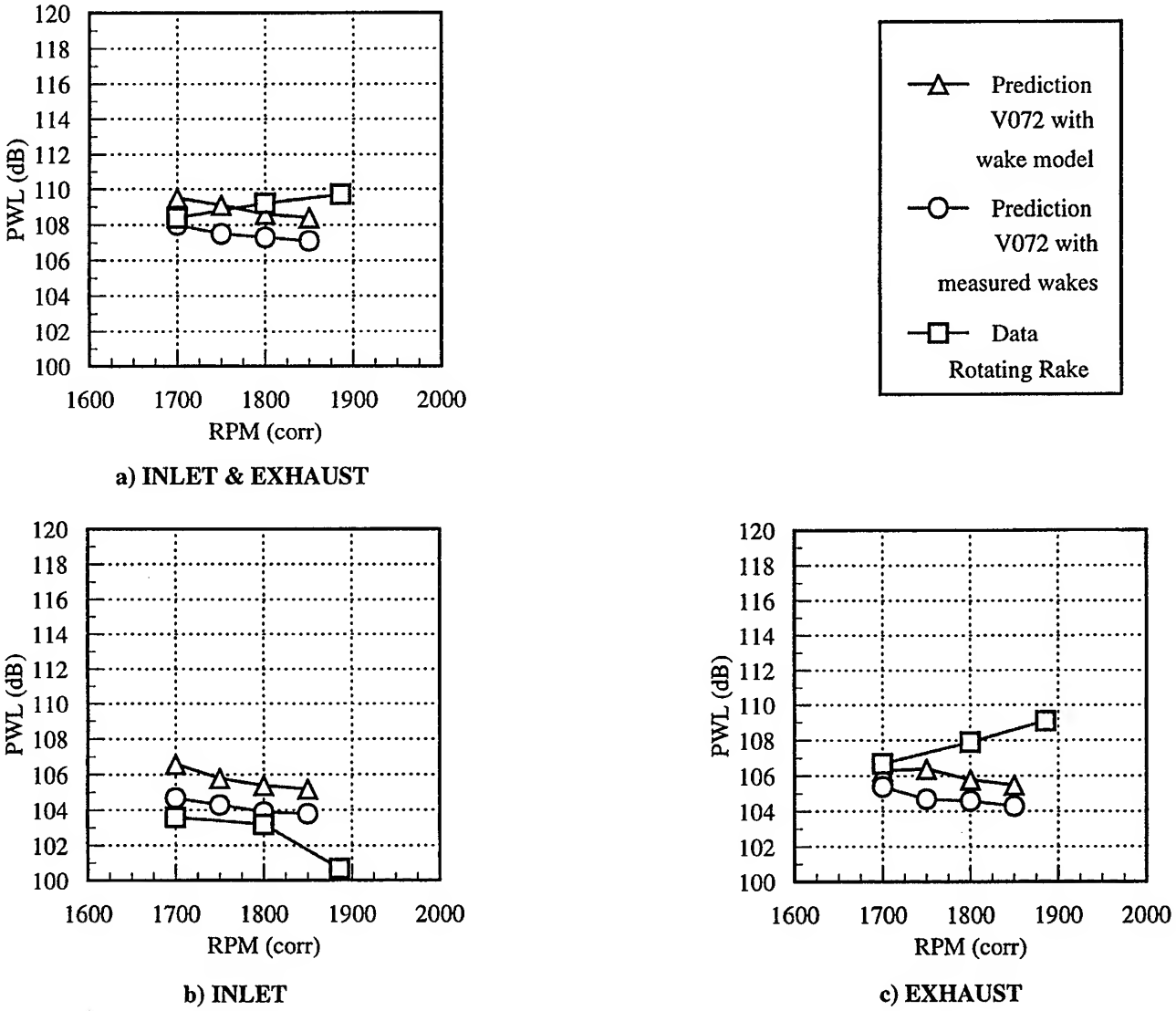

FIGURE 12. Comparisions of Mode Power Levels for 28 Vanes Sum of 2BPF Modes (4,0) & (4,1)

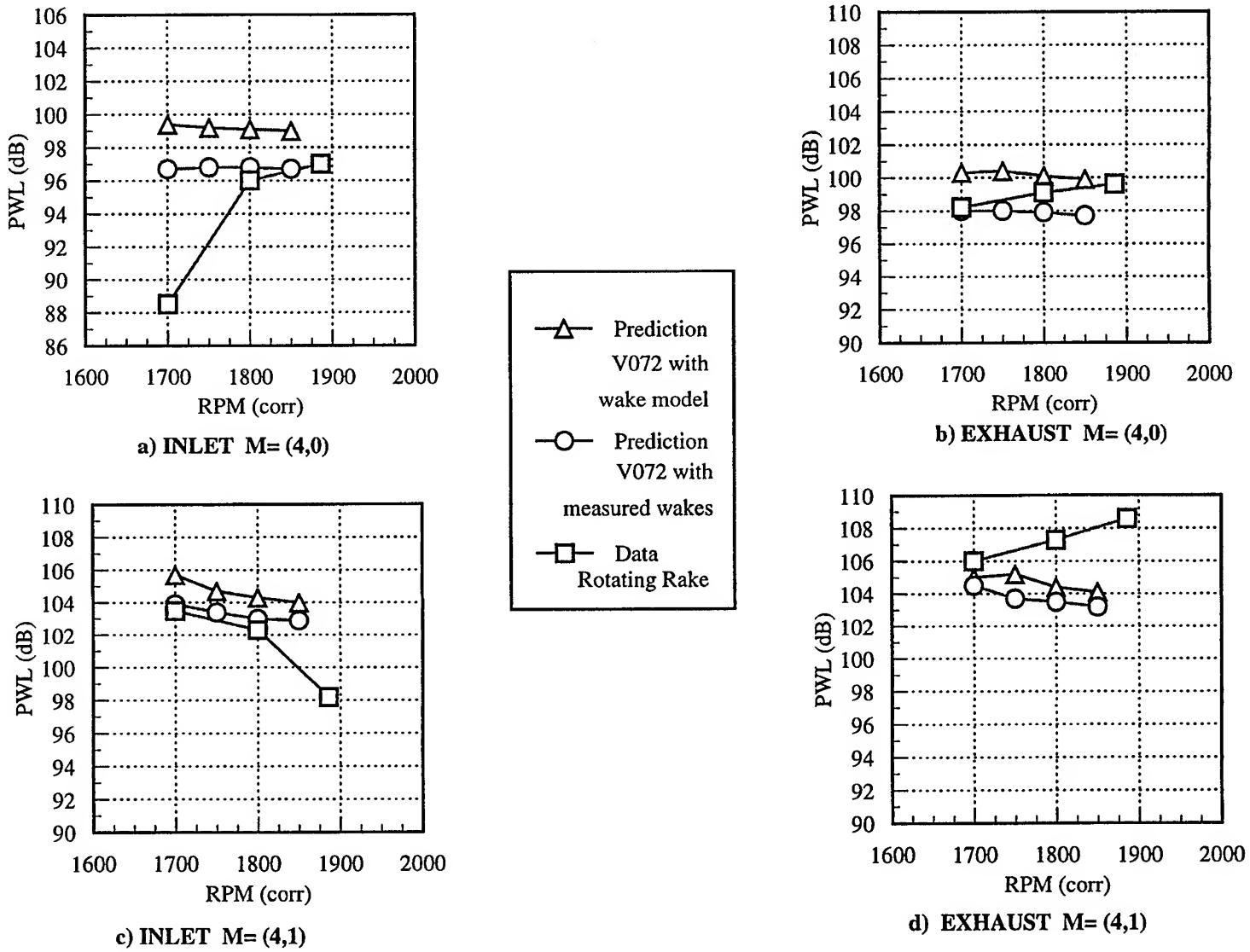

FIGURE 13. Comparisions of Mode Power Levels for 28 Vanes 2BPF Individual Modes (4,0) & (4,1)

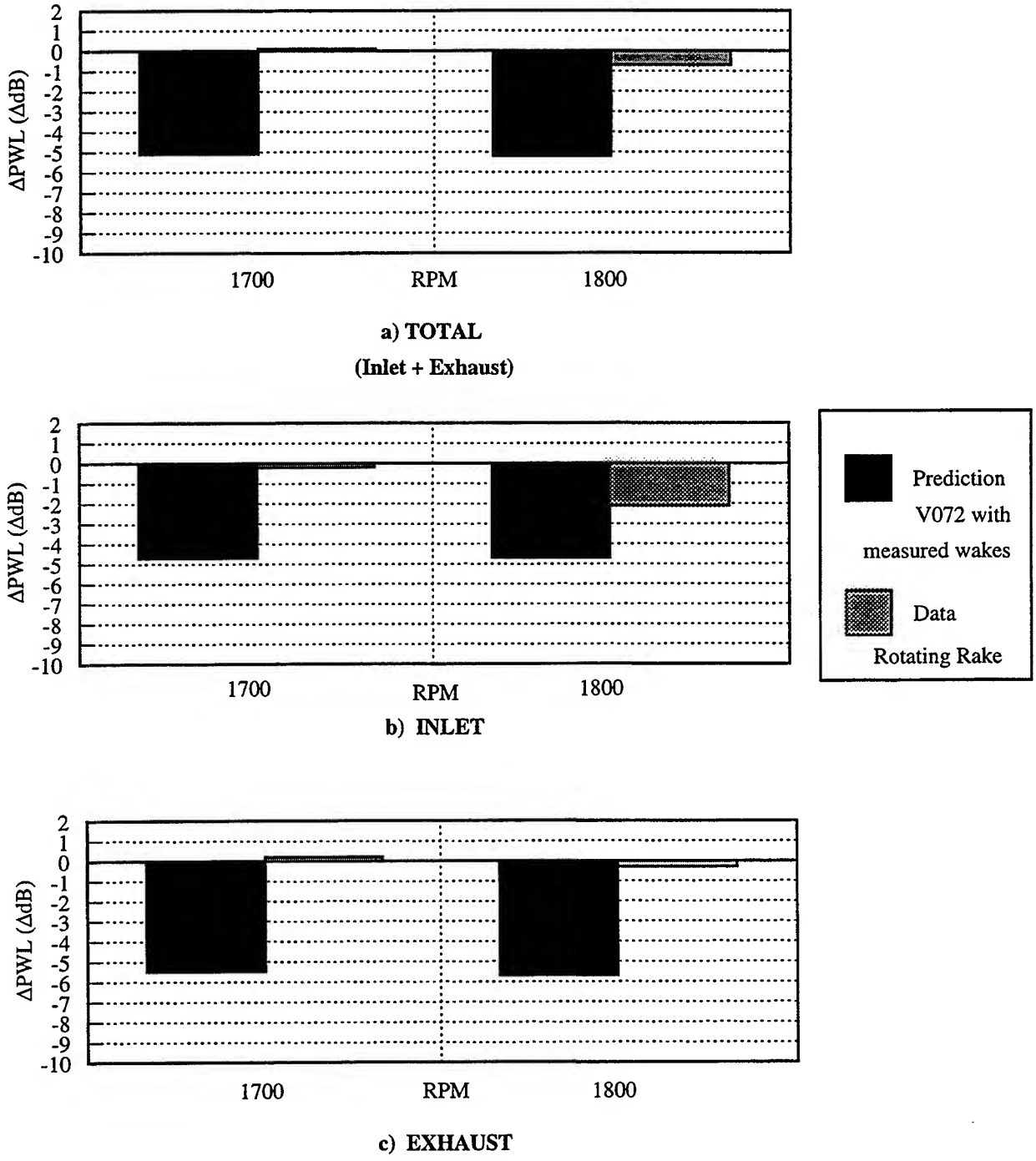

FIGURE 14. Comparisions of Mode Power Level Increments for BPF [14 Vanes Mode (2,0) Amplitude - 13 Vanes Mode (3,0) Amplitude]

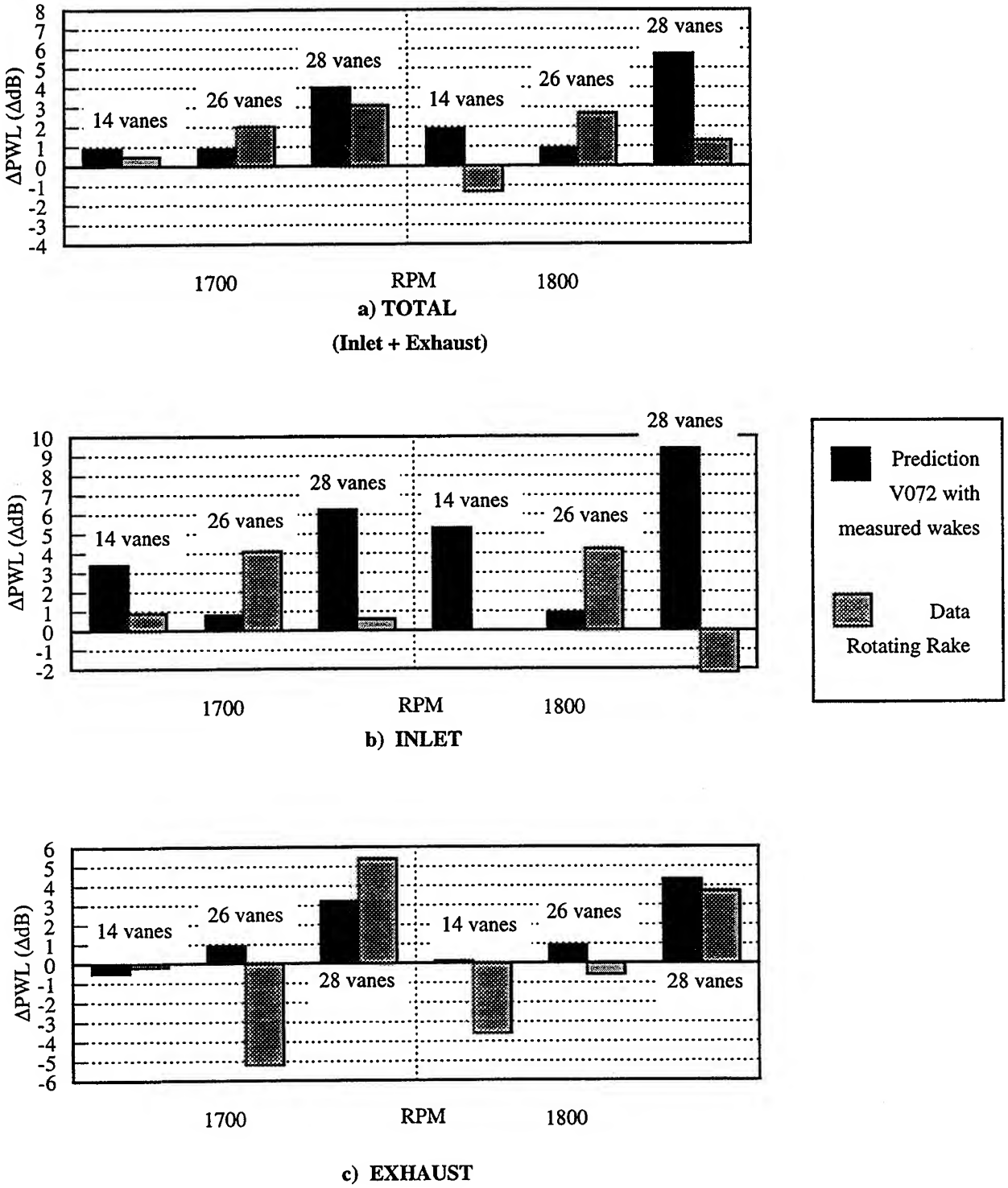

FIGURE 15. Comparisions of Mode Power Level Increments for 2BPF [V Vanes Sum of Mode Amplitudes - 13 Vanes Sum of Mode Amplitudes]

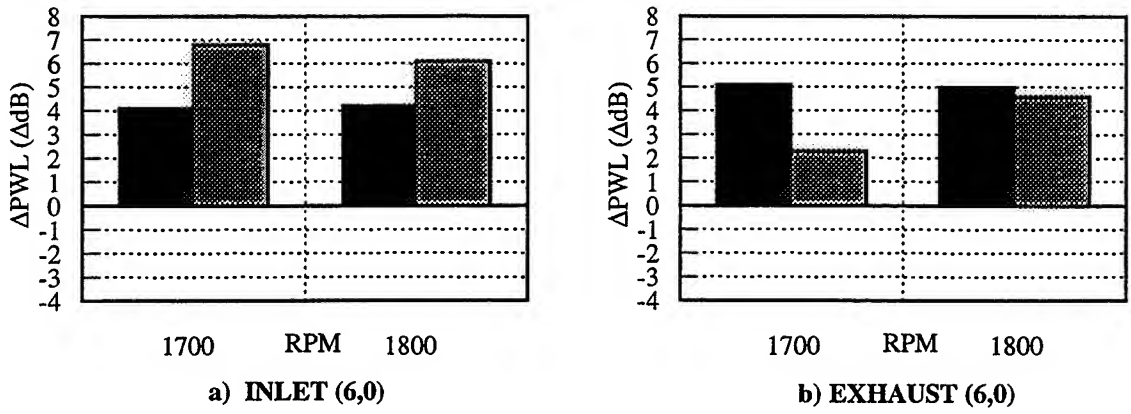

FIGURE 16. Comparisions of Mode Power Level Increments for 2BPF [26 Vanes Mode (6,0) Amplitude - 13 Vanes Mode (6,0) Amplitude]

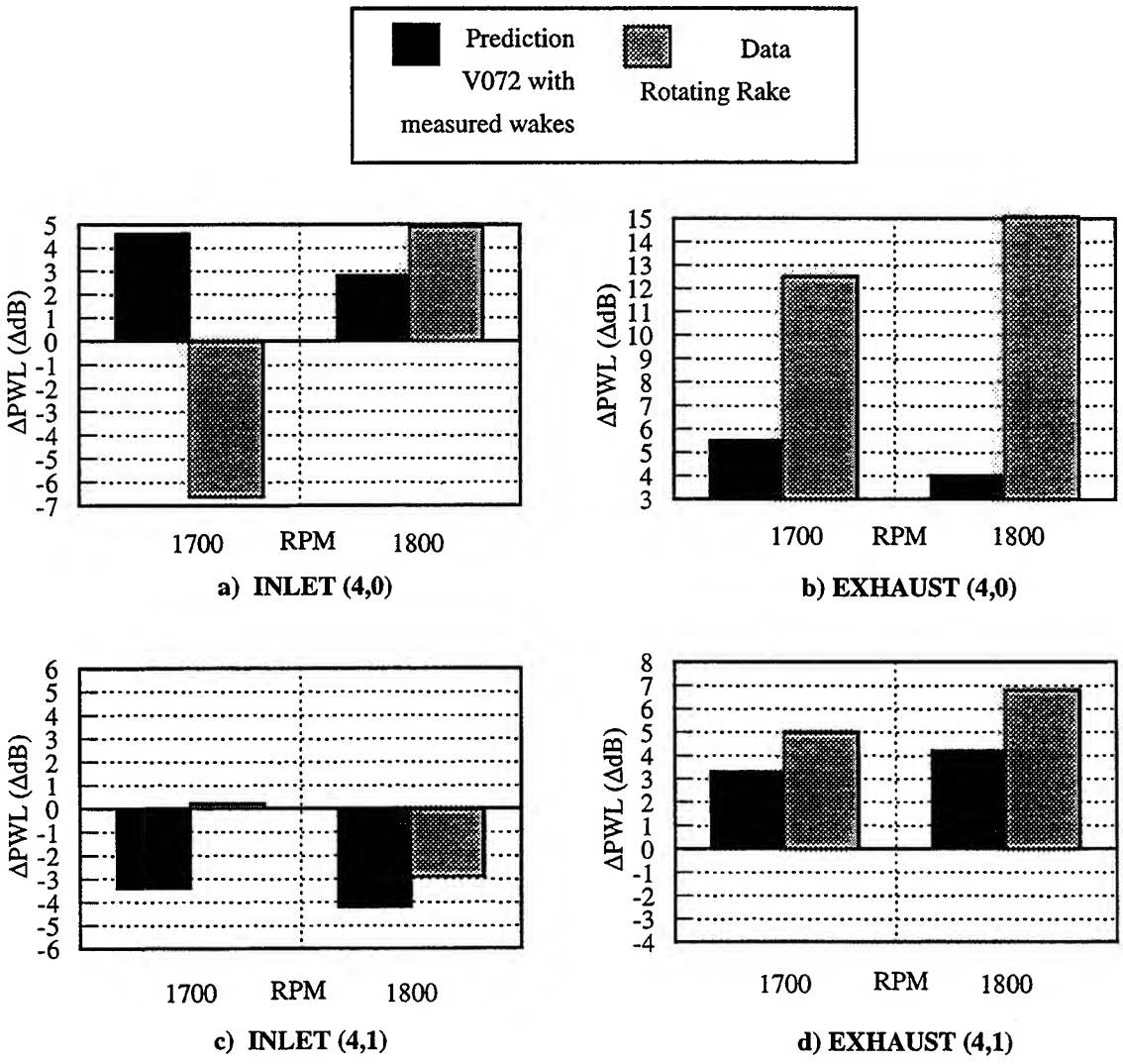

FIGURE 17. Comparisions of Mode Power Level Increments for 2BPF [28 Vanes Mode (4,n) Amplitude - 14 Vanes Mode (4,n) Amplitude]

REPORT DOCUMENTATION PAGE

Form Approved
OMB No. 0704-0188

1. AGENCY USE ONLY (*Leave blank*)	2. REPORT DATE	3. REPORT TYPE AND DATES COVERED
	May 1996	Technical Memorandum

4. TITLE AND SUBTITLE

Comparison of Predicted Low Speed Fan Rotor/Stator Interaction Modes to Measured

5. FUNDING NUMBERS

WU–538–03–11

6. AUTHOR(S)

Daniel L. Sutliff, James Bridges, and Edmane Envia

7. PERFORMING ORGANIZATION NAME(S) AND ADDRESS(ES)

National Aeronautics and Space Administration
Lewis Research Center
Cleveland, Ohio 44135–3191

8. PERFORMING ORGANIZATION REPORT NUMBER

E–10748

9. SPONSORING/MONITORING AGENCY NAME(S) AND ADDRESS(ES)

National Aeronautics and Space Administration
Washington, DC 20546–0001

10. SPONSORING/MONITORING AGENCY REPORT NUMBER

NASA TM–107462
AIAA–97–1609

11. SUPPLEMENTARY NOTES

Prepared for the 3rd Aeroacoustic Conference cosponsored by the American Institute of Aeronautics and Astronautics and the Confederation of European Aerospace Societies, Atlanta, Georgia, May 8–12, 1997. Daniel L. Sutliff, AYT Corporation, 2001 Aerospace Parkway, Brook Park, Ohio 44142 (work funded by NASA Contract NAS3–27571); James Bridges, NASA Lewis Research Center; and Edmane Envia, NYMA, Inc., 2001 Aerospace Parkway, Brook Park, Ohio 44142 (work funded by NASA Contract NAS3–27186). Responsible person, Daniel L. Sutliff, organization code 5940, (216) 433–6290.

12a. DISTRIBUTION/AVAILABILITY STATEMENT

Unclassified - Unlimited
Subject Categories 07 and 71

This publication is available from the NASA Center for AeroSpace Information, (301) 621–0390.

12b. DISTRIBUTION CODE

13. ABSTRACT ***(Maximum 200 words)***

The *V072 Rotor Wake/Stator Interaction Code* is widely used as a state-of-the-art prediction code. This paper validates the code by comparing experimentally measured mode levels to those predicted by V072. The experimental mode levels were measured by the Rotating Rake system installed on the 48" Active Noise Control Fan at NASA Lewis Research Center. V072 predicted mode levels by inputting the actual wake profiles of the ANCF rotor measured by a 2-component hotwire. The mode levels were also predicted from the V072 wake models. V072 reasonably predicts the mode levels within the design limits of the code.

14. SUBJECT TERMS

Ducted fans; Engine noise; Aircraft noise; Aeroacoustics; Acoustic modes

15. NUMBER OF PAGES

23

16. PRICE CODE

A03

17. SECURITY CLASSIFICATION OF REPORT	18. SECURITY CLASSIFICATION OF THIS PAGE	19. SECURITY CLASSIFICATION OF ABSTRACT	20. LIMITATION OF ABSTRACT
Unclassified	Unclassified	Unclassified	